

Analysis of Anisotropic Ionization Coefficient in Bulk 4H-SiC with Full-Band Monte Carlo Simulation

R. Fujita, K. Konaga, Y. Ueoka, Y. Kamakura, and N. Mori
Graduate School of Engineering, Osaka University
2-1 Yamada-oka, Suita, Osaka 565-0871, Japan

T. Kotani
Graduate School of Engineering, Tottori University
4-101 Konan-cho Minami, Tottori 680-8550, Japan

Abstract—High-field electron transport characteristics in bulk 4H-SiC are simulated with the full-band Monte Carlo method, and anisotropy of the ionization coefficient α is discussed. The simulation results exhibit larger α along $\langle 11\bar{2}0 \rangle$ direction than $\langle 0001 \rangle$ direction, which is consistent with the experimental observation. Furthermore, the dependence of α on the electric field direction θ is investigated. Compared to the existing analytical model, the present simulation results show a steeper increase when θ is tilted from the c -axis, which is originated from the anisotropic nature of the hot-electron heating.

I. INTRODUCTION

SiC is an attractive wide-bandgap material for next generation power devices because of its high breakdown field, high saturation velocity, high thermal conductivity, etc. In recent years, 4H-SiC based Schottky barrier diodes (SBDs) and MOSFETs have been commercialized, and the device simulation technology is greatly expected to predict the device characteristics and to optimize the device structure. However, the carrier transport properties in 4H-SiC have not been fully understood yet, which are essential to develop the physical models for accurate device simulation. For example, it has been reported that the ionization coefficient in 4H-SiC shows strong anisotropic behavior [1], and the 2D device simulation predicted that it significantly affects the breakdown voltage of SBDs [2].

In this study, we simulate the high-field electron transport characteristics in bulk 4H-SiC by using a full-band Monte Carlo (FBMC) method, and investigate the anisotropy of the ionization coefficient.

II. SIMULATION METHOD

In this study, the FBMC simulation was performed to investigate the high-field electron transport characteristics in bulk 4H-SiC. The k -space is discretized into equal grids (the region indicated in Fig. 1 was divided into $30 \times 30 \times 10$ grids), and the $E-k$ relationship of the lowest 40 conduction bands is stored as a look-up table.

The electron band structure and impact ionization rate of bulk 4H-SiC to be implemented into the FBMC simulator was calculated based on a hybrid quasiparticle self-consistent

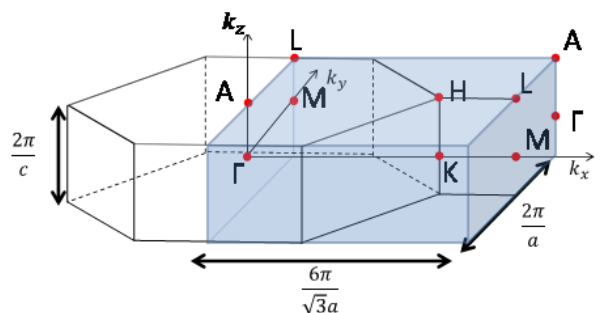


Fig. 1. Schematic view of the k -space region to store the $E-k$ relationship for FBMC simulation (shaded area). The hexagonal cylinder represents the first Brillouin zone of bulk 4H-SiC.

GW (QSGW) method using the ecalj code [3], [4]. By adjusting the mixture ratio of the QSGW and the local density approximation (LDA) results as QSGW : LDA = 79.5 : 20.5, the experimentally observed bandgap energy at 300K ($E_g = 3.26$ eV [5]) was obtained. In Fig. 2, the calculated conduction band structure of bulk 4H-SiC is presented. The effective masses at the conduction band bottom along M- Γ and M-K directions are $0.53 m_0$ and $0.28 m_0$, respectively, which are close to the experimental values ($0.58 m_0$ and $0.29 m_0$ [6]).

The impact ionization rate was calculated also through the QSGW method [7] and implemented into the FBMC simulator as a function of the electron energy E by fitting to the Keldysh formula [8]:

$$P_{ii}(E) = \alpha \left(\frac{E - E_{th}}{E_{th}} \right)^\beta \Theta(E - E_{th}), \quad (1)$$

where Θ is the unit step function, $\alpha = 2.0 \times 10^{11} \text{ s}^{-1}$, $\beta = 3.4$ and $E_{th} = 3.26$ eV.

The acoustic and non-polar optical phonon scatterings were considered in this study. The scattering rates were calculated based on the formula given in [8] using the density of states calculated from the band structure shown in Fig. 2. The acoustic and non-polar optical phonon scattering rates (P_{op}

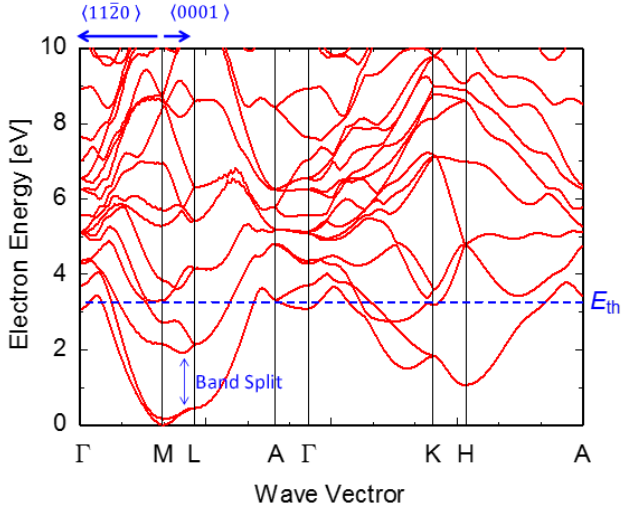


Fig. 2. Conduction band structure of bulk 4H-SiC calculated with the hybrid QSGW method. Impact ionization threshold energy E_{th} is indicated by the dashed line. The conduction band minima is located at the M point.

and P_{ac}) are given by

$$P_{op}(E) = \frac{D_{op}^2 \hbar}{2\rho E_{op} \pi} \left[N(E_{op}) + \frac{1}{2} \mp \frac{1}{2} \right] \text{DOS}(E \pm E_{op}), \quad (2)$$

$$P_{ac}(E) = \frac{D_{ac}^2 k_B T}{\rho \hbar v_s^2 \pi} \text{DOS}(E), \quad (3)$$

where D_{op} and D_{ac} are the acoustic and optical deformation potentials respectively, \hbar is the Planck's constant, ρ is the crystal density, $N(E)$ is the Bose-Einstein distribution, $\text{DOS}(E)$ is the density of the states, k_B is the Boltzmann's constant, T is the lattice temperature, and v_s is the sound velocity. For P_{op} , the upper sign corresponds to phonon absorption and the lower sign to phonon emission. P_{ac} includes absorption and emission. In this model, the acoustic phonon scattering process is assumed to be elastic, while the inelastic optical phonon scattering is considered with a constant optical phonon energy E_{op} . Parameters used in this study are shown in table I. The same parameters as [8] were used except for D_{op} , which was adjusted to reproduce the experimental ionization coefficient. Figure 3 shows the scattering rates plotted as a function of electron energy E .

In order to obtain the ionization coefficient α , the motions of 1,000 electrons were simulated under the homogeneous

TABLE I
PARAMETERS USED TO CALCULATE THE PHONON SCATTERING RATES

D_{ac}	D_{op}	E_{op}	ρ	v_s
[eV]	[eV/cm]	[meV]	[g/cm ³]	[cm/s]
19	7.4×10^{10}	85	3.2	1.4×10^6

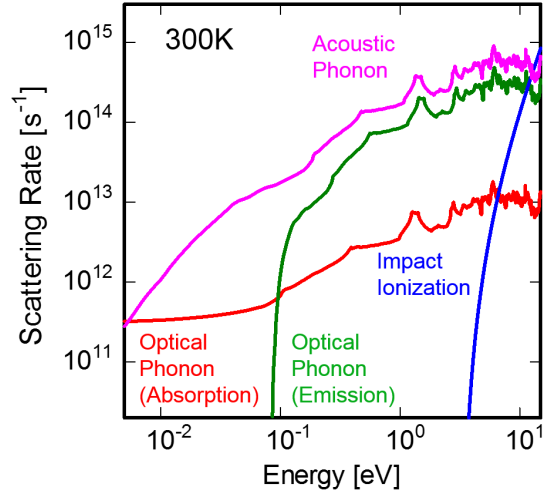


Fig. 3. Electron energy dependence of the scattering rates implemented in the present FBMC simulation.

electric field \mathbf{F} for the simulation time of $t_{sim} = 100$ ps. Then, α was calculated from

$$\alpha = \frac{N_{ii}}{\mathbf{r}_d \cdot \mathbf{F}/|\mathbf{F}|}, \quad (4)$$

where N_{ii} is the average number of impact ionization events per electron and \mathbf{r}_d is the average displacement of electrons during t_{sim} .

III. RESULTS AND DISCUSSION

Figure 4 shows the simulated ionization coefficient α for electrons in bulk 4H-SiC along $\langle 0001 \rangle$ and $\langle 11\bar{2}0 \rangle$ directions plotted together with the experimental data [1], [9]–[13]. In this study, we have adjusted D_{op} to fit the experimental α of [9] measured under high electric field (3–5 MV/cm) applied along $\langle 0001 \rangle$ direction. Note that when the field direction is rotated to perpendicular to the c -axis (i.e., $\langle 11\bar{2}0 \rangle$ direction), significantly larger α was obtained, which was also observed experimentally [1]. Figure 5 shows the ionization coefficient as a function of the electric field angle θ with respect to the c -axis. For comparison, the characteristics based on the analytical formula for the anisotropic impact ionization model [2] are also plotted. The present FBMC simulation results show steeper increase than the analytical model in the low angle region. Figure 6 compares the contour lines of α plotted on the $F_{\perp} - F_{\parallel}$ plane. In the anisotropic impact ionization model [2], it is assumed that the equi- α line has an ellipsoidal shape, while the FBMC simulation result exhibit the tapered shape at the top and the bottom ends indicating α is sensitively dependent on θ when the field is directed to the c -axis.

In the present simulation, the impact ionization rate P_{ii} was assumed to be a function of E and not to depend on the direction of the electron wave vector. Hence, the observed anisotropy of α is originated from the anisotropic nature of

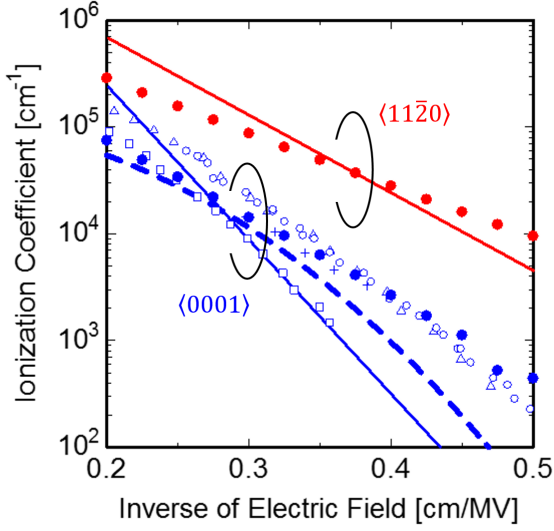


Fig. 4. Simulated ionization coefficient plotted as a function of the inverse of the electric field applied along $\langle 0001 \rangle$ and $\langle 11\bar{2}0 \rangle$ directions (closed dots). Experimental data are indicated by the solid lines [1], the dashed line [9], the open squares [10], the open triangles [11], the crosses [12], and the open circles [13].

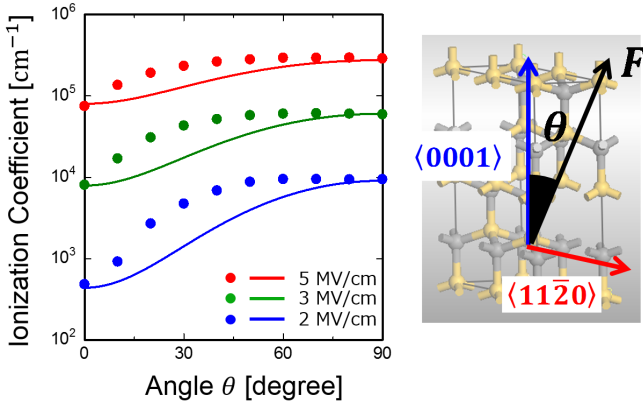


Fig. 5. Ionization coefficient depending on the electric field direction. θ is the angle with respect to the c -axis. The FBMC simulation results (dots) are compared with the analytical anisotropic impact ionization model [1] (lines).

the electron heating. Figure 7 shows the electron distribution in k -space simulated under the homogeneous electric field of 2 MV/cm directed to $\langle 0001 \rangle$ and $\langle 11\bar{2}0 \rangle$ directions. The splitting of the conduction band along M–L direction is considered to suppress the electron transition to higher bands when the electric field is directed to the $\langle 0001 \rangle$ direction [14]. On the other hand, there is no band splitting along M– Γ direction, indicating that the hot electrons are easily generated under the electric field along $\langle 11\bar{2}0 \rangle$ direction. Figure 8 shows the electron energy distributions simulated under the electric field of 2 MV/cm directed to various directions. Note that the high energy tail of the electron distribution increases rapidly when θ is in the low angle region, while it is less dependent on θ larger than $\sim 40^\circ$, which is consistent with the behavior

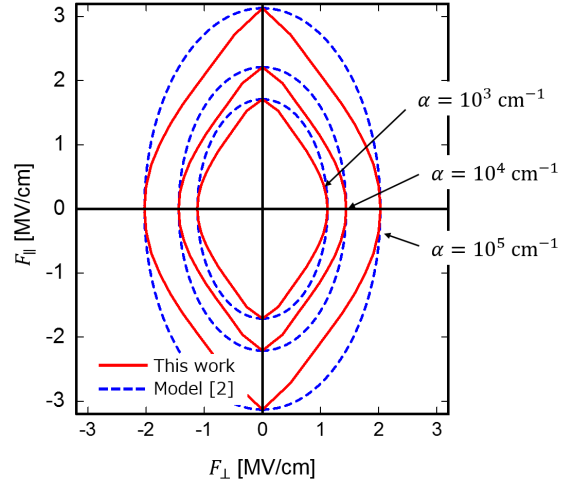


Fig. 6. Contour lines of the ionization coefficient (at $\alpha = 10^3 \text{ cm}^{-1}$, 10^4 cm^{-1} , 10^5 cm^{-1}) plotted on the F_{\perp} – F_{\parallel} plane. The results of this work (solid lines) are compared with the model assumed in [2] (dashed lines).

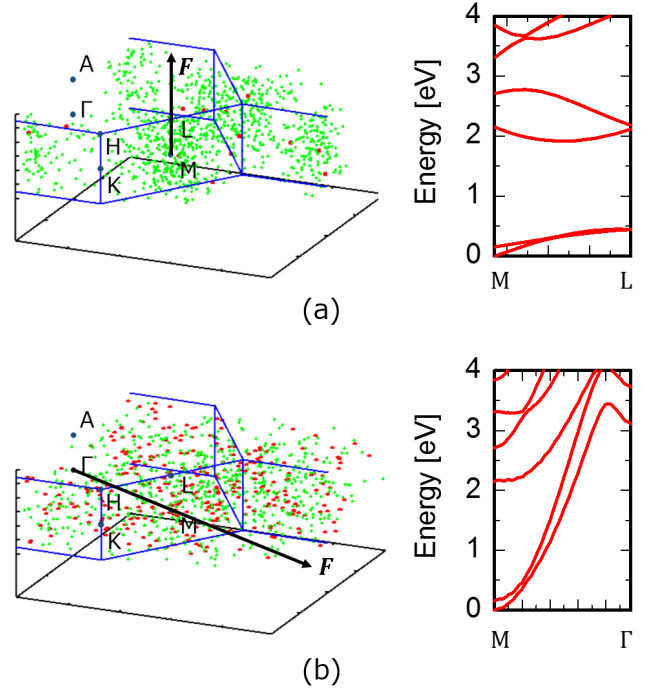


Fig. 7. Electron distribution in k -space simulated under the electric field of 2 MV/cm directed to $\langle 0001 \rangle$ direction (a) and directed to $\langle 11\bar{2}0 \rangle$ directions (b). The red dots show the electrons existing in the first or the second lowest conduction bands, while the green dots are the electrons in the higher conduction bands. The right figures show the conduction band structure plotted along M–L and M– Γ directions.

of α confirmed in Fig. 5.

IV. CONCLUSION

We have simulated the high-field electron transport characteristics in bulk 4H-SiC with the FBMC method, and discussed

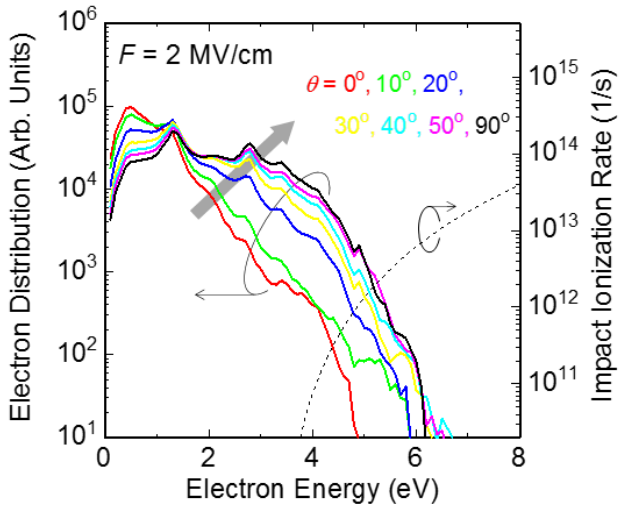


Fig. 8. Electron energy distributions simulated under the electric field of 2 MV/cm directed to various directions (solid lines). Impact ionization rate is indicated by the dashed line.

the anisotropy of the ionization coefficient α . The simulation results showed the larger α along $\langle 11\bar{2}0 \rangle$ direction than $\langle 0001 \rangle$ direction, which is consistent with the experimental observation. Furthermore, the dependence of the ionization coefficient on the electric field direction θ was investigated. Compared to the existing analytical model, the present simulation results of α showed the steeper increase with θ tilted from the c -axis, which is originated from the anisotropic nature of the hot-electron heating.

ACKNOWLEDGMENT

This work was supported by the Semiconductor Technology Academic Research Center (STARC).

REFERENCES

- [1] T. Hatakeyama, T. Watanabe, T. Shinohe, K. Kojima, K. Arai, and N. Sano, "Impact ionization coefficients of 4 H silicon carbide," *Appl. Phys. Lett.*, vol. 85, pp. 1380–1382, 2004.
- [2] T. Hatakeyama, J. Nishino, C. Ota, and T. Shinohe, "Physical Modeling and Scaling Properties of 4H-SiC Power Devices," *Proc. 2005 SISPAD*, pp. 171–174, 2005.
- [3] T. Kotani, "Quasiparticle self-consistent GW method based on the augmented plane-wave and muffin-tin orbital method," *J. Phys. Soc. Jpn.*, vol. 83, pp. 0974711-1–0974711-11, 2014.
- [4] D. Deguchi, K. Sato, H. Kino, and T. Kotani, "Accurate energy bands calculated by the hybrid quasiparticle self-consistent GW method implemented in the ecalj package," *Jpn. J. Appl. Phys.*, vol. 55, pp. 051201-1–051201-8, 2016.
- [5] T. Kimoto and J.A. Cooper., *Fundamentals of Silicon Carbide Technology* (Wiley, Singapore, 2014).
- [6] P. Käckell, B. Wenzien and F. Bechstedt., "Influence of atomic relaxations on the structural properties of SiC polytypes from ab initio calculations," *Phys. Rev. B*, vol. 50, pp. 17037–17048, 1994.
- [7] T. Kotani and M. van Schilfgaarde, "Impact ionization rates for Si, GaAs, InAs, ZnS, and GaN in the GW approximation," *Phys. Rev. B*, vol. 81, pp. 125201-1–125201-5, 2010.
- [8] A. Akturk, N. Goldsman, S. Potbhare, and A. Leis, "High field density-functional-theory based Monte Carlo: 4H-SiC impact ionization and velocity saturation," *J. Appl. Phys.*, vol. 105, pp. 033703-1–033703-7, 2009.

- [9] H. Niwa, J. Suda, and T. Kimoto, "Impact Ionization Coefficients in 4H-SiC Toward Ultrahigh-Voltage Power Device," *IEEE Trans. Electron Devices*, vol. 62, pp. 3326–3333, 2015.
- [10] A.O. Konstantinov, Q. Wahab, N. Nordell, and U.Lindefelt, "Ionization rates and critical field in 4H-SiC," *Appl. Phys. Lett.*, vol. 71, pp. 90–92, 1997.
- [11] W.S. Loh et al., "Impact ionization coefficients in 4H-SiC," *IEEE Trans. Electron Devices*, vol. 55, pp. 1984–1990, 2008.
- [12] R. Raghunathan and B.J. Baliga., "Measurement of electron and hole impact ionization coefficients for SiC," *Proc. IEEE ISPSD*, pp. 173–176, 1997.
- [13] B.K. Ng, "Impact ionization in wide band gap semiconductors: $\text{Al}_x\text{Ga}_{1-x}\text{As}$ and 4H-SiC," Ph.D. dissertation, Univ. Sheffield, Sheffield, U.K., 2002.
- [14] S. Nakamura, H. Kumagai, T. Kimoto, and H. Matsunami, "Anisotropy in breakdown field of 4H-SiC," *Appl. Phys. Lett.*, vol. 80, pp. 3355–3357, 2002.
- [15] M. Hjelm, H-E. Nilsson, A. Martinez, K.F. Brennan, and E. Bellotti, "Monte Carlo study of high-field carrier transport in 4H-SiC including band-to-band tunneling," *J. Appl. Phys.*, vol. 93, pp. 1099–1107, 2003.
- [16] T. Kunikiyo, M. Takenaka, Y. Kamakura, M. Yamaji, H. Mizuno, M. Morifuji, K. Takaguchi, and C.Hamaguchi, "A Monte Carlo simulation of anisotropic electron transport in silicon including full band structure and anisotropic impact-ionization model," *J. Appl. Phys.*, vol. 75, pp. 297–312, 1994.